Efficiency of surface shaping for protection of leading edges in the divertor of ASDEX Upgrade from direct plasma exposure

K. Krieger[1,*], J.W. Coenen[2], D. Brida[1], Y. Gao[2], J.P. Gunn[3], A. Hakola[4], A. Herrmann[1], T. Lunt[1], S. Potzel[1], B. Sieglin[1], ASDEX Upgrade Team, EUROfusion MST1 Team[*]

[1]*Max-Planck-Institut für Plasmaphysik, Garching, Germany*
[2]*Forschungszentrum Jülich, IEK - Plasmaphysik, Jülich, Germany*
[3]*CEA, IRFM, Saint Paul Lez Durance, France*
[4]*VTT Technical Research Centre of Finland Ltd, P.O.Box 1000, VTT, Finland*

Melting of tungsten plasma-facing components (PFCs) in tokamaks may occur either by transient heat flux excursions due to plasma instabilities or by excessive power loads to leading edges at gap side faces of PFCs exposed to the parallel power flux. Minimising potential melt damage requires, apart from mitigation of excessive transient power loads, a PFC design with optimised surface shaping to shadow PFC and castellation side faces from the parallel power flux. Code predictions of the shadowing efficiency based on 3D modelling of single particle trajectories, including gyro orbit motion but neglecting the sheath electric field [1], indicate that for typical castellation shadowing depths < 0.5 mm, hot ions, which become expelled during an ELM and flow down to the divertor target plates, may penetrate a geometrically shadowed area because their gyro orbit radius is comparable to the shadow depth (e.g. in ITER, with ELM energies $E_{i,ELM}$ = 5 keV and a toroidal field of B_t = 6 T, the gyro radius is r_L = 2.4 mm while typical shaping elevations are ≈ 0.5 mm). For typical ITER ELM parameters the resulting transient power flux to otherwise shadowed edges could, according to these simulations, exceed the tungsten damage thresholds.

To assess the validity of the simulations' underlying physics model, the predicted shadow penetration effect was studied in ASDEX Upgrade using ITER baseline type-I ELMy H-mode discharges, which provide ELM ion energies of 400-700 eV according to their typical plasma pedestal temperatures [2]. Despite their lower energy, their gyro radius is similar to that of corresponding ITER ELM ions because the toroidal magnetic field in the ASDEX Upgrade discharges is B_t = 2 T so that for $E_{i,ELM}$ = 0.4 keV, r_L = 2 mm. Due to the toroidally tilted installation of the outer divertor target tiles with an upstream edge elevation of 0.8 mm ASDEX Upgrade provides shadowed zones at the outer divertor with a toroidal width of ≈ 8 mm (Figure 1) and a depth similar to planned shaping steps at the ITER target castellations. Finally, the magnetic field angle of incidence is also comparable in both ITER and ASDEX Upgrade (Figure 2). Code predictions for the ASDEX Upgrade geometry and plasma conditions using the 3D ion orbit model suggested observable penetration effects during type I ELMs. To validate the predicted effect, the power flux to a customised target

[*] *see http://www.euro-fusionscipub.org/mst1*

tile was measured by infra-red thermography with sub-mm lateral resolution (Figure 3) [3]. In addition, two adjacent sample tiles equipped with a 20 nm W-marker layer were exposed using the divertor manipulator DIM-II [4]. This allowed quantifying the lateral distribution of W erosion both inside and outside of the shadowed zone by Rutherford backscattering analysis of the layer thickness pre- and post-exposure. The poloidal variation of W gross erosion was measured spectroscopically by quantitative observation of the WI 400.9 nm spectral line emission at the sample tile surface.

The thermal response of the tile surface was measured by the IR camera with a frame rate of 1 kHz and an exposure time of 13 μs per frame. Because the ELMs in these discharges have a duration of about 1 ms, analysis of a single ELM event could not provide conclusive evidence. Therefore, in a first analysis step, the IR response at three representative toroidal image positions was quantified by coherent averaging over all ELMs in the discharge #31697. Figure 4 shows the resulting time traces of the IR response ≈ 25 mm above the strike line for a point in the plasma exposed part of the surface, a point just inside the shadowed area of the surface and, for comparison, for a point inside the gap between adjacent tiles. The signal originating from the tile gap should not show any effect due to ELM impact safe for IR volume emission from the plasma fan above the target plate. Indeed, one observes significant IR emission following the actual ELM impact with a duration well beyond that of the actual ELM with a duration of ≈4 ms. This contribution is also seen in the signals from the actual tile surface and is approximately toroidally uniform. It is attributed to bremsstrahlung emitted by the high density cool divertor plasma built up transiently by the recycling particles of the ELM pulse. The effect is further amplified by the IR system's viewing geometry with a line of sight approximately tangentially along the divertor plasma fan. In contrast, the IR transient due to the actual ELM is in the shadowed surface zone by a factor of 6-10 lower than in the plasma exposed surface fraction. Still, Figure 4 clearly shows evidence for penetration of hot ELM ions into the magnetically shadowed zone, however, at a significantly lower fraction than predicted by the numerical simulations based on the simple 3D single particle model. Figure 4 also demonstrates that the IR time resolution allows to analyse the IR response to ELM impact by comparing single thermography image frames before an ELM and just after ELM impact. An example is given in Figure 5, which shows the toroidal profile of the surface temperature increase right after ELM onset at a time of t = 1.994 s. Also shown is the expected temperature increase according to the ion orbit simulations (red curve) as well as the extent of the geometric shadow (blue curve). While the simulation predicts a transient power flux due to hot ELM ions at approximately 40% of the power flux delivered to the plasma exposed surface fraction, the IR measurement yields an upper limit of about 10%. This is in line with the measured thickness change of the W-marker tile, which shows clear erosion near the strike point zone in the plasma exposed tile area, while in the shadowed area no erosion is seen within the experimental error.

For the discrepancy there are a number of potential causes. One reason could be the lack of electrical field drifts in the 3D orbit model. The influence of that simplification was studied for the ITER geometry and parameter space by PIC simulations [5], which also took into account possible collective mechanisms and sheath effects not included in the single particle model. However, these simulations revealed no significant discrepancies to the simple 3D orbit model. Another effect leading to the observed weaker penetration fraction might be the energy transfer from ELM electrons to ions during their passage from upstream to the divertor, which, in the free streaming ELM model [6], is required to maintain quasi-neutrality [7]. If the ions arriving at the target plate have significantly larger parallel energy than their perpendicular thermal energy, a correspondingly larger fraction will have passed the shadowed zone before their gyromotion leads to impact at the shadowed surface.

In conclusion the ASDEX Upgrade experiments demonstrate that hot ELM ions indeed can penetrate magnetically shadowed zones at shaped plasma facing surfaces. However, the resulting transient power loads to shadowed areas are smaller than predicted in simulations. Further experimental analysis is on the way to assess the consequences for predictive modelling of the power loads at ITER target plate module concepts with shaped castellations.

References

[1] J. Gunn et al., *Surface Heat Loads on Tungsten Monoblocks in the ITER Divertor*, Proc. of the 25th IAEA Fusion Energy Conf. 2014, FIP/1-2, 499, Saint Petersburg, Russia.

[2] J. Schweinzer et al., *Development of the Q=10 Scenario for ITER on ASDEX Upgrade*, Proc. of the 25th IAEA Fusion Energy Conf. 2014, EX/9-4, 169, Saint Petersburg, Russia.

[3] B. Sieglin et al., *Real Time Capable IR Thermography for ASDEX Upgrade*, subm. to Rev. Sci. Instr.

[4] A. Herrmann et al., *A large divertor manipulator for ASDEX Upgrade*, Fus. Eng. and Design, in press (2015), doi:10.1016/j.fusengdes.2015.02.007.

[5] M. Komm et al., *Particle-in-cell simulations of heat loads on ITER divertor monoblocks during steady-state and transient plasma conditions*, 15th Int. Conf. on Plasma Facing Mat. & Comp., Aix-en-Provence, 2015.

[6] T. Eich et al., J. of Nucl. Mat. **390-391** (2009) 760-763.

[7] Ch. Guillemot et al., *Experimental estimation of tungsten impurity sputtering due to Type I ELMs in JET-ITER-like Wall*, 15th Int. Conf. on Plasma Facing Mat. & Comp., Aix-en-Provence, 2015.

Acknowledgement

This work has been carried out within the framework of the EUROfusion Consortium and has received funding from the Euratom research and training programme 2014-2018 under grant agreement No 633053. The views and opinions expressed herein do not necessarily reflect those of the European Commission.

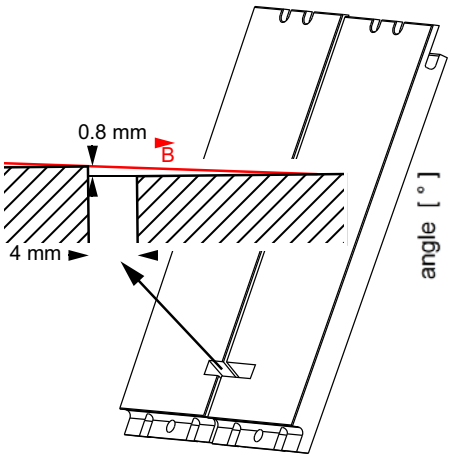

Figure 1: *Outer divertor tiles with cross-section showing magnetic shadowing.*

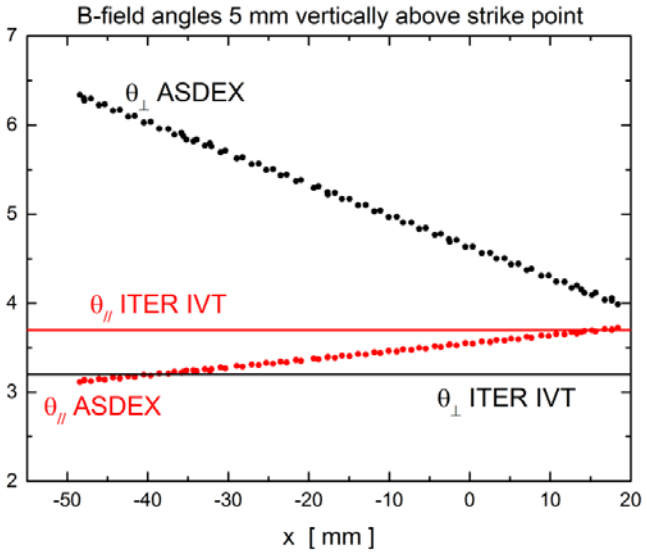

Figure 2: *Field line poloidal pitch angle, $\theta_{||}$, and angle to tile surface, $\theta_{\perp}$, for ITER and ASDEX Upgrade #31697.*

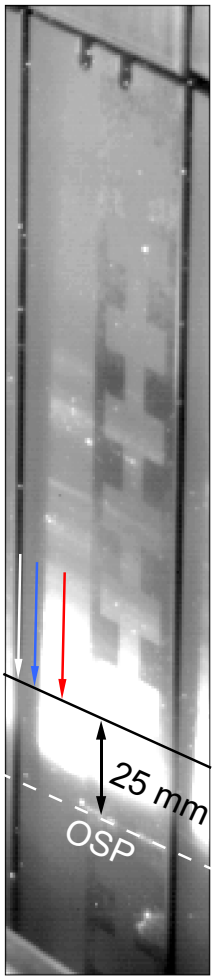

Figure 3: *Outer divertor tile observed by thermography camera with locations for coherent average of ELMs (Figure 4).*

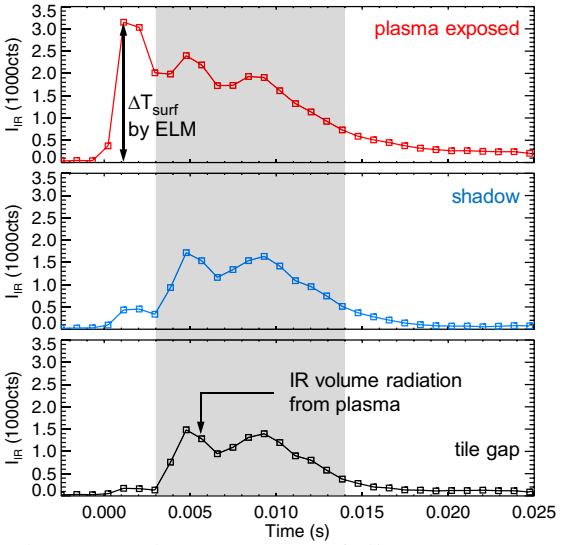

Figure 4: *Coherent average of all ELM transients in #31697 at 3 points 25 mm above strike line.*

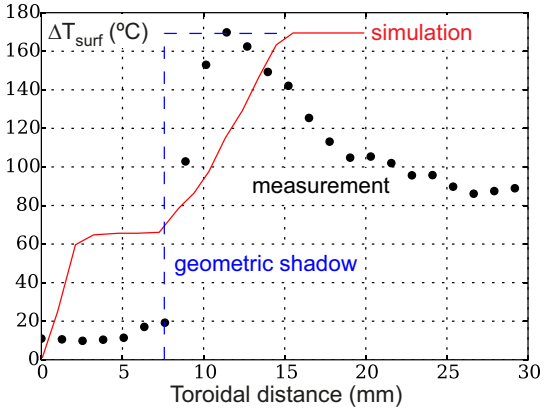

Figure 5: *Toroidal profile of ΔTsurf by ELM at t=1.994 s, 10 mm above strike line in #31697.*